


Research Article

Honey-Processed *Chelidonium majus* L. Ameliorates OVA-Induced Allergic Asthma Through Energy Metabolism and Inflammation Regulation

Renguang Wang¹, Xintong Sui¹, Xin Dong¹, Liming Hu¹, Zhimeng Li¹, Guoxin Ji¹, Shumin Wang^{1,*} 

¹College of Pharmacy, Changchun University of Chinese Medicine, 130117 Changchun, Jilin, China

*Correspondence: wangsm@ccucm.edu.cn (Shumin Wang)

Academic Editor: Mehmet Ozaslan

Published: 30 August 2025

Abstract

Background and Objective: Allergic asthma, a chronic respiratory illness, presents a significant healthcare burden. Honey-processed *Chelidonium majus* L. (HC), a traditional herbal formula, has shown promise as an anti-asthmatic treatment. However, the underlying mechanisms for these properties remain elusive. Thus, this study aimed to investigate the therapeutic potential and mechanisms of HC in a rat model of ovalbumin (OVA)-induced asthma. **Materials and Methods:** Sprague-Dawley rats were randomly assigned to Control, Model (asthma), Dexamethasone (positive control), low-, medium-, and high-dose HC groups (n = 8). Lung histopathology, serum inflammatory marker (interleukin (IL)-10, IL-13, and IL-1 β), serum metabolomics, and transcriptomic analyses were employed to assess the effects of HC on airway inflammation, mucus hypersecretion, and related metabolic and gene expression profiles. **Results:** HC treatment alleviated histological lung injury in asthmatic rats, downregulated the levels of proinflammatory cytokines (IL-13 and IL-1 β), while upregulating the anti-inflammatory cytokine IL-10. Metabolomic analysis revealed 46 metabolic biomarkers while the transcriptome analysis identified 754 differentially expressed genes (DEGs) between the Model and Control groups. Moreover, 35 metabolites were reversed and 273 DEGs were identified following high-dose HC treatment. Integration analysis manifested that 7 DEGs and 11 metabolites were associated with several enriched metabolic pathways, including amino acid metabolism, fatty acid metabolism, glycometabolism, organic acid metabolism, and nucleotide metabolism. **Conclusion:** HC treatment ameliorates OVA-induced asthma in rats by regulating the expression of specific genes to restore metabolic homeostasis and suppress inflammation. This study provides valuable insights into the therapeutic potential and mechanisms of HC for asthma treatment.

Keywords: *Chelidonium majus*; honey-processed; ovalbumin-induced allergic asthma; metabolomics; transcriptomics; inflammatory respiratory disorder

1. Introduction

Asthma is a chronic inflammatory respiratory disorder that is influenced by a combination of hereditary and environmental variables [1]. It is usually induced by various allergens and characterized by chronic airway inflammation, airway hyperresponsiveness (AHR) and airway remodeling [2,3]. Asthma is caused mainly by an imbalanced ratio of T helper type 1 (Th1) to Th2 cells, contributing to the T cells differentiating into Th2 cells. The Th2 lymphocytes can produce Th2 cytokines, which recruit multiple inflammatory cells and lead to airway inflammation [4–6].

Chronic airway inflammation is the key to the pathogenesis of asthma and is also the basis of airway remodeling and AHR [7]. Interleukin (IL)-13, a Th2 cytokine, plays a critical role in eosinophilic inflammation, airway remodeling and AHR [8]. As a pro-inflammatory cytokine, the cytokine IL-1 β , which is mainly secreted by macrophages, participates in airway inflammatory infiltration, promotes Th2 cytokine release [9], Th17 inflammatory responses [10] and initiates airway smooth muscle hyper-reactivity

[11]. The IL-10 is a powerful inhibitor of pro-inflammatory cytokine production [12]. It has also been reported that inflammatory cytokines like IL-13 and IL-1 β induce mucus hypersecretion [8,13].

Scientific statistics have shown that over 300 million people worldwide suffer from asthma [14]. While corticosteroids, β -agonists and antihistamines are mainstay treatments for asthma, their limitations, including a lack of cure and potential side effects [15], necessitate the exploration of novel therapeutic options as complementary or alternative medicines for asthma treatment. Some traditional Chinese medicine (TCM) preparations have exhibited good therapeutic effects in treating asthma [16,17]. A nationwide study in Taiwan demonstrated reduced asthma hospitalization for school-aged children receiving long-term Chinese herbal medicine therapy [18].

A perennial herb in the Papaveraceae family, *Chelidonium majus* L. (greater celandine), boasts a long history in treating various ailments, such as asthma, bronchitis and inflammatory disorders [19]. Pharmacological



interest stems from its diverse bioactive profile, encompassing alkaloids (e.g., sanguinarine, chelidonine and chelerythrine), flavonoids and phenolic acids [20–22]. These constituents contribute to its anti-inflammatory, antioxidant, immunomodulatory, antitumor and antispasmodic properties [21,23–31]. A study using an asthma-induced mouse model have shown that *C. majus* extracts can inhibit eosinophil proliferation and activation, suggesting their therapeutic potential [32]. Furthermore, chelidonine, the main alkaloid in *C. majus*, effectively reduced eosinophilic airway inflammation by suppressing the production of key inflammatory mediators like IL-4 and eotaxin-2 in an allergic asthma mouse model [32,33]. These findings suggest *C. majus* as a promising therapeutic agent for asthma. However, potential limitations exist. Some *C. majus* components may exhibit potential mild toxicity and many factors, like processing methods, can influence their efficacy. Further research to optimize processing techniques is crucial to address these limitations.

The TCM practitioners have long utilized processing techniques to refine crude herbs, aiming to improve their therapeutic efficacy and minimize potential toxicity [34, 35]. Processing methods encompass diverse techniques, including cleansing, size reduction, stir-frying and utilization of liquid additives [36]. Research has demonstrated that processing significantly alters the chemical profiles of herbal medicines, consequently impacting their pharmacological activity [37,38]. While processing boasts a rich tradition, the mechanisms behind processing's effects on most herbal medicines remain unclear. Recent studies have begun to unveil some of these mechanisms, including the reduction of toxic components, chemical transformations of active ingredients, increased solubility, physical alterations of the constituents and potential interactions with added excipients. Honey possesses multiple biological activities, including anti-inflammatory, antioxidant, antifungal and antibacterial properties [39–41]. As an alternative medicine, honey is used to treat asthma by Malaysians [42]. Processing with honey is a common practice in TCM herbal preparation. Understanding how this processing influences the mechanisms of action of these herbal medicines is essential for standardizing processing methodologies and ensuring the safety and effectiveness of herbal medicines in clinical practice. Further research is needed to explore the therapeutic mechanisms of processed herbal medicines and develop optimized processing methods. Therefore, considering the promise of *C. majus* for treating asthma and the potential advantages associated with honey processing in TCM, investigating the therapeutic mechanism of honey-processed *C. majus* (HC) for asthma holds significant promise.

Despite promising preclinical evidence suggesting the therapeutic potential of *C. majus* for allergic asthma, its clinical application is limited by concerns regarding its potential toxicity and variable efficacy. This study explored honey-processed *C. majus* (HC) as a potential strat-

egy to address these limitations. The *C. majus* was processed with honey and metabolomics and transcriptomics were employed to investigate asthma-relevant metabolic profile changes, molecular hallmarks of asthma and molecular mechanisms involved in HC treatment. By investigating the therapeutic potential of HC, this work is expected to contribute to the development of improved asthma treatments with enhanced safety and efficacy. Therefore, this study investigated the therapeutic potential and mechanisms of HC in a rat model of ovalbumin (OVA)-induced asthma.

2. Materials and Methods

2.1 Study Area

The experiments were conducted in the Microorganism and Biochemical Pharmacy Innovation Lab at College of Pharmacy, Changchun University of Chinese Medicine, during March to October, 2021.

2.2 Preparation of Methanol Extract From HC

Dexamethasone (Dex) and ovalbumin (OVA) were obtained from Suicheng Pharmaceutical Co., Ltd. (Zhengzhou, China) and Shanghai Yuanye Bio-Technology Co., Ltd. (Shanghai, China), respectively. *Chelidonium majus* samples were provided by Hebei Renxin Pharmaceutical Co., Ltd. (Hebei, China). The botanical identity of the samples was confirmed by Prof. Shumin Wang of Changchun University of Chinese Medicine. The honey-processing procedure for *Chelidonium majus* was conducted following the general rules of the Chinese Pharmacopeia 2020 Edition [43]. Refined honey was subjected to dilution using boiling water at a boiling water/refined honey ratio of 1:1.9 (w/w).

After stirring of obtained mixed sample (20.7:100, diluted honey/raw *C. majus*, w/w) till total moistening, the sample was put in a preheated pan, followed by mild fire frying to dryness. Before being stored in a desiccator, the honey-processed *C. majus* (HC) was cooled in the plate. The HC was ground into a powder and sieved through a 60 mesh filter. The precisely weighed powder (400 g) was subjected to reflux extraction with 80% methanol for two 1 hr cycles. After conflating, the filter liquor was concentrated under reduced pressure, freeze-dried into powder and finally storage at –80 °C.

2.3 Ultra-Performance Liquid Chromatography-Quadrupole-Executive Orbitrap Mass Spectrometry (UPLC-Q-Exactive MS) Analysis of HC Extract

The HC extract was dissolved in a solution of methanol containing 2-amino-3-(2-chloro-phenyl)-propionic acid (4 ppm) and was then passed through a 0.22 µm membrane. Composition identification was performed on a Vanquish UHPLC System (Thermo Fisher Scientific, Waltham, MA, USA) coupled with a Q-Exactive Focus

mass spectrometer (Thermo Fisher Scientific, Waltham, MA, USA) equipped with an electrospray ionization (ESI) source [44]. The detailed instrument parameters for UPLC-Q-Exactive MS analysis are provided in **Supplementary Table 1**.

Composition was initially confirmed based on accurate molecular weight (MW error ≤ 30 ppm) and subsequently obtained by annotating mzCloud, PubChem, LipidMaps and Human Metabolome Database (HMDB) based on MS/MS fragmentation patterns [45,46].

2.4 Animal Handling

Specific pathogen-free (SPF) male Sprague-Dawley (SD) rats (220 ± 20 g) were obtained from Changchun Yisi Laboratory Animal Technology Co., Ltd. (Changchun, China). The rats were housed in plastic cages under 22 ± 2 °C, $50 \pm 5\%$ humidity and 12/12 hrs light/dark cycle conditions. All animal experimentation procedures adhered to the guidelines and were approved by the Animal Ethics Committee of Changchun University of Chinese Medicine (protocol No.: 2020345; approval date: October 11, 2020).

Forty-eight rats were randomized as 6 groups ($n = 8$): Control, Model (asthma), Dexamethasone (Dex, positive control) and low, medium and high-dose HC (HCL, HCM and HCH) groups. An asthma model was established after 7 days of routine feeding. The sensitizing solution was prepared by dissolving 100 mg OVA and 100 mg aluminum hydroxide in 1 mL of normal saline. Rats in each group (except control) received intraperitoneal injections of sensitization solution on days 1 and 8. Control rats were given injections of 1 mL of normal saline in an identical way. Following the last sensitization (day 15), each group was continuously gaged for 7 days. The Control and Model groups received normal saline, the Dex group received dexamethasone (0.5 mg/kg) and the HC groups received their respective doses (0.81, 1.21 or 1.62 mg/kg) according to the regulations of Chinese Pharmacopoeia 2020 Edition [43]. The gavage volume was 10 mL/kg/day. Thirty minutes after each administration, the rats were challenged with 1% (w/v) OVA solution in a plexiglass chamber for 30 min once daily. Likewise, normal saline was given to control rats.

2.5 Pulmonary Histopathology

Following the final atomization inhalation, rats were fasted for 12 hrs. The next day, they were deeply anesthetized under intraperitoneal sodic pentobarbital anesthesia (100 mg/kg). After confirming the absence of a pedal reflex, the rats were euthanized via exsanguination or thoracotomy. A portion of lung tissue was collected for pathological analysis. After fixation with 4% paraformaldehyde, the lung tissues were dehydrated in ethylic alcohol, embedded in paraffin and sliced (4 μ m). Hematoxylin and Eosin (H&E) staining was performed with sections for assessing inflammation. Periodic acid-Schiff (PAS) staining was performed to evaluate goblet cell hyperplasia. A scoring system (0–4 scale) was adopted to evaluate the severity of peri-

bronchial and perivascular inflammation, while goblet cell hyperplasia was graded (0–4 scale) based on the number of PAS-positive cells in each airway [47,48]. Masson staining was employed for assessing collagen fiber deposition in airways, which stained blue. ImageJ software version 1.54 (NIH, Bethesda, MD, USA) was utilized to quantify the percentage of collagen fiber area [49]. A double-blind approach was employed for the evaluation of inflammation.

2.6 Enzyme-Linked Immunosorbent Assay (ELISA)

Serum samples were collected and the supernatant was subjected to centrifugation (3000 rpm, 10 min, 4 °C). The concentrations of inflammatory mediators (IL-10, IL-13 and IL-1 β) were quantified according to the instructions of ELISA kits. Commercial kits for measuring rat IL-10 (MM-0176M2), IL-13 (MM-089802) and IL-1 β (MM-0040M2) were offered by Jiangsu Meimian Industrial Co., Ltd., Yancheng, China.

2.7 Serum Metabolomic Profiling

Serum samples from the Control, Model and HCH groups were subjected to metabolomic analysis utilizing a Waters Acquity UPLC I-Class PLUS (Waters, Medford, MA, USA) with a Waters Xevo G2-XS QTOF mass spectrometer (Waters, Medford, MA, USA) (**Supplementary Table 2**) [50].

Raw data were processed with Progenesis QI software version 3.0 (Nonlinear Dynamics, Wilmslow, UK) for peak extraction, alignment, or additional data implementation, with mass deviation and theoretical fragment identification within < 100 ppm.

Identified metabolites were subsequently searched in established databases (KEGG, LipidMaps and HMDB) to retrieve pathway and classification information. Differential multiples between groups were calculated and statistically evaluated utilizing Student's *t*-tests. To visualize overall separation between groups, Principal Component Analysis (PCA) was employed. Orthogonal projection to latent structures-discriminant analysis (OPLS-DA) modeling was completed using R language package ropls. The model reliability was assessed through 200-fold permutations and model variable importance projection (VIP) was determined through multiple cross-validation. Differentially accumulated metabolites (DAMs) were identified (fold change, FC > 1 , VIP > 1 , $p < 0.05$). Subsequently, pathway enrichment analysis of identified metabolic biomarkers (impact > 0 , $-\log P > 1$) was utilized using MetaboAnalyst 5.0. The significance of KEGG pathway enrichment was determined using a hypergeometric test.

2.8 Transcriptome Analysis

This work collected lung tissues from Control ($n = 3$), Model ($n = 3$) and HCH groups ($n = 3$) for RNA sequencing. The quality and quantity of the isolated RNA were analyzed with a NanoDrop 2000 spectrophotometer (Thermo Fisher Scientific, Waltham, MA, USA). The RNA integrity

Table 1. Primers for target gene expression analysis.

Gene name	Forward primer	Reverse primer
<i>IL6</i>	GAGTTGTGCAATGGCAATTCTG	ACGGAAGTCCAGAAGACCAGAG
<i>IL10</i>	AGAAGCTGAAGACCCTCTGGATA	TTCATTTTGAGTGTACGTAGGC
<i>Ccl2</i>	TTCAAAACAGACCTGCGCTTC	ATGGATAGCACACAGGTTGGTATCT
<i>Cxcl6</i>	TTGACCCAGAAGCTCCGTTG	TGCAAGTGCATTCCGCTTTG
<i>Cxcl2</i>	CTGTACTGGTCCTGCTCCTCCT	AGTGGCTATGACTTCTGTCTGGG
<i>Ptgs2</i>	CTGATGACTGCCCAACTCCC	CTGGGCAAAGAATGCGAACA
<i>Pla2g16</i>	GATATGTGATCCACCTGGCTCC	GTTCAGAGGCAGCGGAGTGTA
<i>Entpd8</i>	TCCCTGAACTACACCCAGAACCT	CATAGAACTGGCCATGCACG
<i>Pde3a</i>	CAGCATAAAGCCACATGAAGCC	ACAGCATAGGACGAAGTGAAGGAC
<i>Pde5a</i>	AAGCAGGCAAGATTGAGAACAAG	CTGGGCTGTTTGAACCATCAA
<i>Pde7b</i>	GGCTCTACCCGTTTCATTGACT	GTCCAAGGTAGTCTTCGTCCAGC
<i>P4ha1</i>	AGATCCAGAAGGGTTTGTCTCGG	CAACCTGGTCTTCGTCTGTTAGG
<i>Adcy9</i>	TGAGACCTTCGGTTACCATTTCC	GACCTCACCTGAGACATGACAAAC
<i>Pck2</i>	TGCCATGGCTGCTATGTACC	TTTGGATGCTACGGCATGGT
<i>Rrm2b</i>	TTTCAGTACCTGGTAAACAAGCC	ATGACTGCAAATCGTGATACTC
<i>Actb</i> (β -actin)	GCGCTCGTCGTCGACAACGG	GTGTGGTGCCAAATCTTCTCC

Notes: Hub genes: *IL6*, *IL10*, *Ccl2*, *Cxcl6*, *Cxcl2* and *Ptgs2*; Key genes: *Pla2g16*, *Entpd8*, *Pde3a*, *Pde5a*, *Pde7b*, *P4ha1*, *Adcy9*, *Pck2*, *Rrm2b* and *Ptgs2*; Reference gene: *Actb* (β -actin).

was evaluated utilizing an Agilent Bioanalyzer 2100 system (Agilent Technologies, Santa Clara, CA, USA) with an RNA Nano 6000 Assay Kit. The cDNA libraries were constructed and their quality was verified using an Agilent Bioanalyzer 2100 system (Agilent Technologies, Santa Clara, CA, USA). Raw reads were further processed using BMK-Cloud platform [51].

Differential gene expression analysis was performed using the DESeq2 R package with the criteria of $p < 0.05$ and $|\log_2(\text{FC})| > 1$. Gene functions were annotated using the KEGG Ortholog (KO) database. A protein-protein interaction (PPI) network was constructed for differentially expressed genes (DEGs) commonly identified in the Model-vs-Control and HCH-vs-Model comparisons based on the STRING database (interaction score > 0.7), followed by importing in Cytoscape 3.9.1 software (Cytoscape Consortium, San Diego, CA, USA) for network visualization. The CytoNCA plugin was employed to count node topological parameters within the PPI network for identifying hub genes.

2.9 Real-Time Quantitative PCR (RT-qPCR) Analysis

To validate the mRNA expression levels of hub genes, RT-qPCR was employed. Total RNA was isolated from lung tissues utilizing TRIzol reagent (Cat. No. 15596026, Thermo Fisher Scientific, Waltham, MA, USA). The mRNA levels were quantified using SYBR Green Premix Ex TaqII (Cat. No. RR820A, TaKaRa, Dalian, China). The cycling conditions were 95 °C for 30 sec, then 40 cycles of 95 °C for 15 sec and 60 °C for 30 sec. The relative levels of gene expression were calculated by reference to the β -actin level in each sample. Each sample was analyzed with triplicate biological replicates and triplicate technical repli-

cates per biological replicate. The $2^{-\Delta\Delta C_t}$ method was employed to calculate the relative expression levels of genes, and primer sequences are provided in Table 1.

2.10 Integrated Transcriptomics and Metabolomics Analysis

To elucidate the mechanism by which HCH alleviates OVA-induced asthma, 35 metabolic biomarkers and 273 DEGs were coanalyzed using the Cytoscape 3.9.1 software (Cytoscape Consortium, San Diego, CA, USA) plugin Metscape 3.1.3 (University of Michigan, Ann Arbor, MI, USA) to generate a compound-reaction-enzyme-gene network. Spearman's rank correlation coefficients were calculated between 35 metabolic biomarkers and 273 DEGs to identify key genes and metabolites with significant correlations. For validation purposes, RT-qPCR was conducted to verify mRNA levels of 8 key genes and primer sequences were shown in Table 1.

2.11 Data Analysis

Data were represented as Mean \pm Standard Error of the Mean (SEM). GraphPad Prism 8 (GraphPad Software Inc., San Diego, CA, USA) was utilized to analyze pharmacodynamic profiles. One-way ANOVA was employed to assess inter-group differences ($p < 0.05$).

3. Results

3.1 Characterization of HC Extract by UPLC-Q-Exactive MS

The UPLC-Q-Exactive MS analysis was performed to identify the chemical constituents present in the HC extract. This analysis revealed 28 compounds (Supplementary Fig. 1A,B). Under positive ion mode, 21 compounds were

Table 2. 28 identified compounds in HC extract using UPLC-Q-Exactive MS analysis under positive and negative ion modes.

	No.	t _R /min	Identification	Molecular formula	Experimental mass (MS)	Theoretical mass (m/z)	Fragment ion (MS/MS) m/z
Positive ion mode	1	1.364	Chelidonic acid	C ₇ H ₄ O ₆	185.0081	185.0081	141.0181, 97.0288, 96.0447
	2	1.511	p-Coumaric acid	C ₉ H ₈ O ₃	165.0546	165.0546	148.0757, 120.0811, 119.0493, 91.0547
	3	1.936	Caffeic acid	C ₉ H ₈ O ₄	181.0495	181.0495	163.0623, 135.9564, 117.0703, 111.0444, 98.9846, 89.0389, 79.0547
	4	3.463	Magnocurarine	C ₁₉ H ₂₄ NO ₃ ⁺	314.1747	314.1751	269.1179, 175.0756, 143.0492, 107.0495
	5	3.834	Magnoflorine	C ₂₀ H ₂₄ NO ₄ ⁺	342.1698	342.17	299.1275, 297.1119, 282.0882, 279.1026, 269.1169, 265.0857, 237.0907
	6	3.91	Chelamine	C ₂₀ H ₁₉ NO ₆	370.1283	370.1285	352.1193, 321.0754, 291.0649
	7	4.591	Protopine	C ₂₀ H ₁₉ NO ₅	354.1333	354.1336	336.1220, 206.0813, 189.0783, 188.0704, 149.0597
	8	4.732	Chelidonine	C ₂₀ H ₁₉ NO ₅	354.1334	354.1336	336.1230, 323.0912, 305.0805, 275.0700
	9	4.779	Tetrahydrocoptisine	C ₁₉ H ₁₇ NO ₄	324.1227	324.123	307.0960, 249.0906, 188.0702, 176.0705, 149.0596
	10	4.816	Coptisine	C ₁₉ H ₁₄ NO ₄ ⁺	320.0916	320.0917	318.0760, 292.0966, 277.0733, 262.0861
	11	4.9	Homochelidonine	C ₂₁ H ₂₃ NO ₅	370.1648	370.1649	352.1540, 336.1226, 290.0934, 275.0698, 188.0704
	12	5.171	Berberine	C ₂₀ H ₁₈ NO ₄ ⁺	336.1228	336.123	321.0986, 320.0914, 306.0758, 292.0964, 278.0805
	13	5.318	Quercetin	C ₁₅ H ₁₀ O ₇	303.0498	303.0499	302.0432, 301.0338, 257.0441, 229.0493
	14	5.364	Chelerythrine	C ₂₁ H ₁₈ NO ₄ ⁺	348.1227	348.123	333.0977, 332.0914, 318.0759, 290.0813
	15	5.659	Chelilutine	C ₂₂ H ₂₀ NO ₅ ⁺	378.1335	378.1336	363.1097, 362.1008, 348.0862, 332.0912, 320.0918
	16	5.767	Kaempferol	C ₁₅ H ₁₀ O ₆	287.0548	287.055	285.0520, 165.0181, 153.0180
	17	5.86	Isorhamnetin	C ₁₆ H ₁₂ O ₇	317.0655	317.0656	318.0737, 151.0388, 107.0860
	18	7.121	Oxysanguinarine	C ₂₀ H ₁₃ NO ₅	348.0864	348.0866	333.0627, 320.0911, 319.0810, 305.0679, 275.0589, 262.0859, 248.0707, 247.0627, 291.0851
	19	8.496	Dihydrochelerythrine	C ₂₁ H ₁₉ NO ₄	350.1384	350.1387	335.1138, 334.1070, 319.1196, 290.0860
	20	8.62	Dihydrosanguinafine	C ₂₀ H ₁₅ NO ₄	334.1072	334.1074	319.0828, 318.0757, 304.0984, 276.1017
	21	8.621	Corysamine	C ₂₀ H ₁₆ NO ₄ ⁺	334.1063	334.1074	319.0829, 304.0984, 276.1016, 261.0776
Negative ion mode	1	0.693	Citric acid	C ₆ H ₈ O ₇	191.0199	191.02	173.0091, 147.0299, 129.0193, 87.0088, 85.0295
	2	1.468	Gallic acid	C ₆ H ₇ O ₅	169.0143	169.014	125.0295, 97.0295, 81.0346
	3	4.338	Ferulic acid	C ₁₀ H ₁₀ O ₄	193.0508	193.051	178.0262, 134.0685, 133.0648, 118.0415, 106.0735, 105.0702
	4	5.666	Genistein	C ₁₅ H ₁₀ O ₅	269.0458	269.046	225.0559, 201.0560, 151.0041
	5	5.727	Luteolin	C ₁₅ H ₁₀ O ₆	285.0407	285.041	257.0449, 241.2173, 151.0036
	6	5.889	Calycosin	C ₁₆ H ₁₂ O ₅	285.0756	285.076	270.0522, 253.0493, 225.0544, 214.0621, 213.0545, 137.0233
	7	6.181	Formononetin	C ₁₆ H ₁₂ O ₄	267.0664	267.066	253.0462, 252.0428, 251.0353, 224.0464, 223.0409, 195.0443, 132.0222

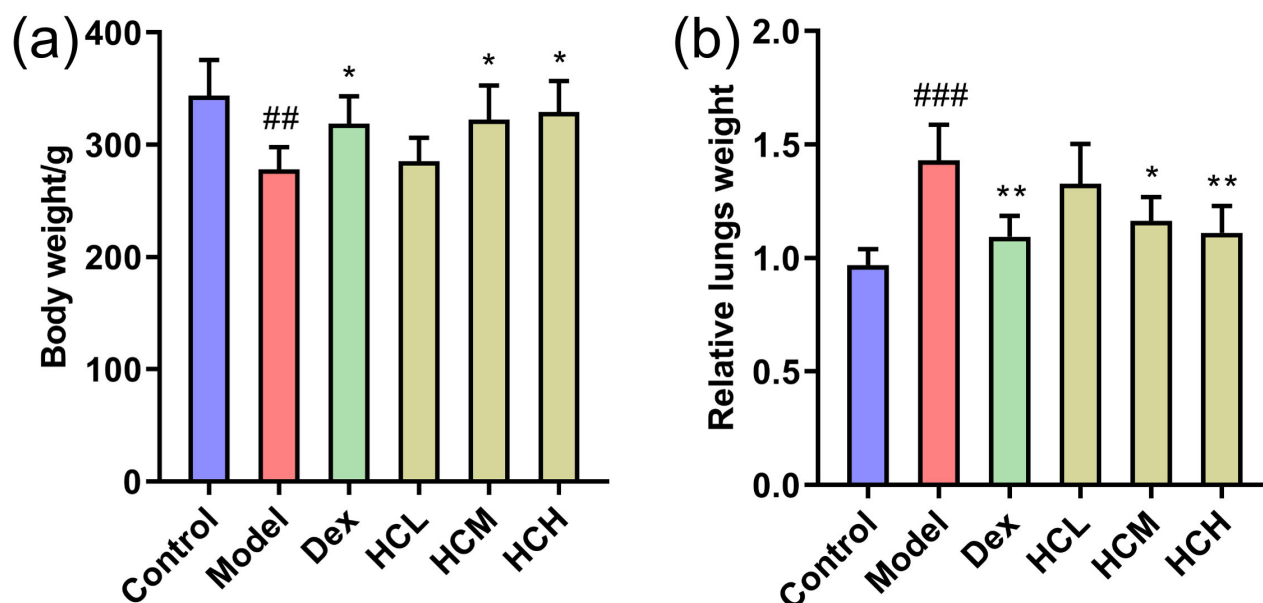


Fig. 1. Effect of HC administration on body weight and relative lung weight in OVA-induced asthmatic rats. (a) Body weight and (b) Relative lung weight of groups after administration. Values are shown as Mean \pm SEM (n = 8), ## p < 0.01, ### p < 0.01 vs Control group and * p < 0.05, ** p < 0.01 vs Model group.

identified, including chelidonic acid, p-coumaric acid, caffeic acid, magnocurarine, magnoflorine, chelamine, propine, chelidonine, tetrahydrocoptisine, coptisine, homochelidonine, berberine, quercetin, chelerythrine, chelilutine, kaempferol, isorhamnetin, oxysanguinarine, dihydrochelerythrine, dihydrosanguinafine and corysamine.

In negative ion mode, 7 compounds were identified, including citric acid, gallic acid, ferulic acid, genistein, luteolin, calycosin and formononetin (Table 2). Further analysis of these identified compounds using the Traditional Chinese Medicine Systems Pharmacology Database and Platform (TCMSP) and relevant literature exploration suggested that all 28 compounds were considered major contributors to the therapeutic effects of HC extract.

3.2 HC Increased Body Weight and Decreased Relative Lung Weight in OVA-Induced Asthmatic Rats

At the start of the experiment, there were no notable differences in body weight and relative lung weight among rats in all six groups. Compared to Control group, OVA challenge caused a notable decrease (p < 0.01) in body weight whereas a remarkable increase (p < 0.001) in relative lung weight in Model group. Administration of Dex, medium- and high-dose HC (HCM and HCH) remarkably elevated body weight (p < 0.05) whereas suppressed (p < 0.01, p < 0.05 and p < 0.01) relative lung weight compared to Model group (Fig. 1a,b).

3.3 HC Relieved Histopathological Changes

Histological examination of bronchial tissues revealed no abnormalities in the Control group. In contrast, the

Model group displayed marked infiltration of inflammatory cells in bronchi and perivascular. Administration of Dex, HCM and HCH obviously reduced the severity of inflammatory cell infiltration compared to Model group (Fig. 2a). Based on PAS staining, there was few goblet cells in Control group. On the contrary, the Model group displayed significant proliferation of goblet cells on airway epithelium. The Dex, HCL, HCM and HCH groups obviously attenuated goblet cell proliferation compared to the model group (Fig. 2b).

3.4 HC Ameliorates Inflammatory Markers in OVA-Induced Asthma Model

In Model group, IL-13 and IL-1 β levels were notably elevated, while IL-10 level was lower in comparison to Control group. Inversely, compared to Model group, treatment with Dex, HCM and HCH reduced IL-13 and IL-1 β levels and notably increased IL-10 levels. The HCL group also significantly reduced IL-1 β and increased IL-10 levels (p < 0.05) compared to Model group (Fig. 3a–c). These findings demonstrated that medium- and high-dose HC exerted anti-inflammatory effects, with high-dose HC potentially exhibiting a more pronounced effect.

3.5 Metabolomic Profile of HCH Treatment in OVA-Induced Asthma Model

To assess the stability of the UPLC-MS method, three quality control (QC) samples, prepared by pooling equal aliquots of experimental samples from all groups, were run before initiating the experiment and then once every six samples throughout the analysis. Furthermore, polar and

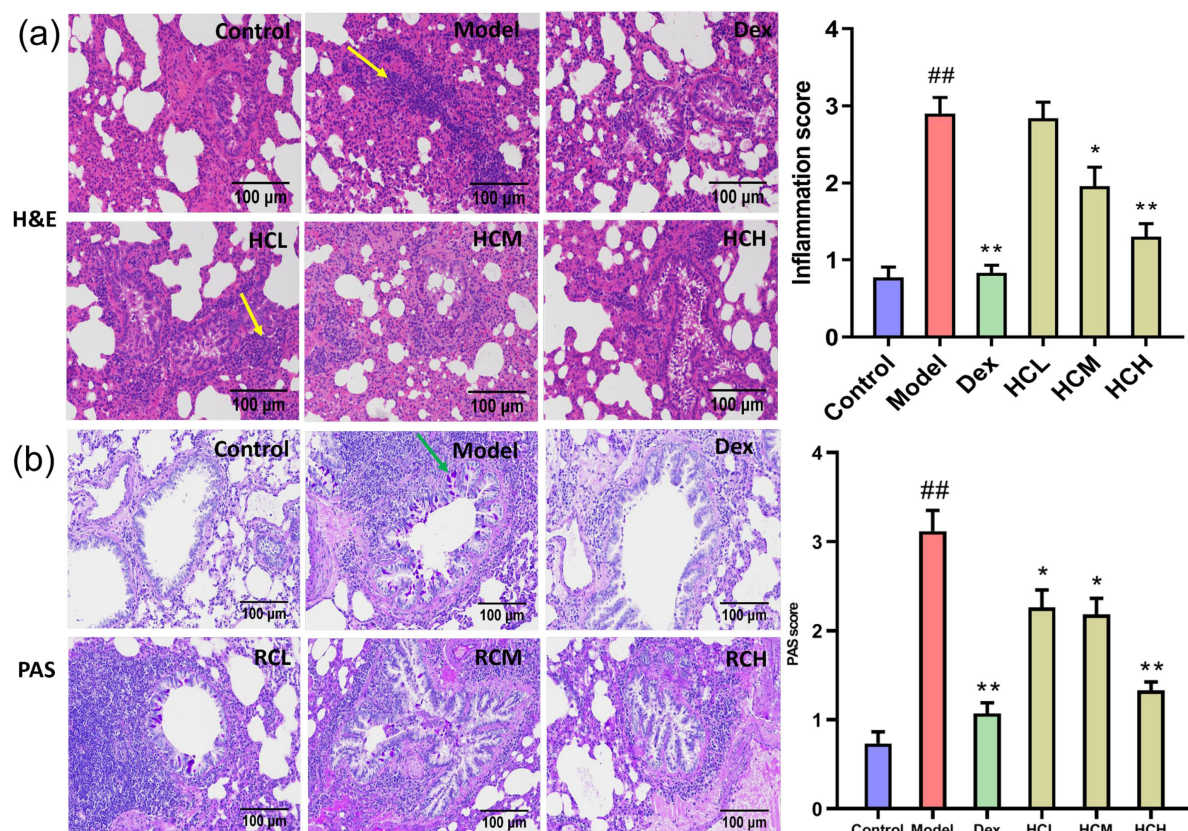


Fig. 2. HC alleviates pulmonary inflammation and goblet cell proliferation. (a) Hematoxylin and Eosin (H&E) staining of lung sections ($\times 200$) and inflammation scores and (b) Periodic acid-Schiff (PAS) staining of pulmonary sections ($\times 200$) and the PAS score. Scale bar = 100 μ m. (a) Yellow arrows indicate goblet cell proliferation and (b) Green arrows indicate inflammatory cell infiltration. Data are represented as Mean \pm SEM ($n = 3$), ^{##} $p < 0.01$ vs Control group and $^*p < 0.05$, $^{**}p < 0.01$ vs Model group.

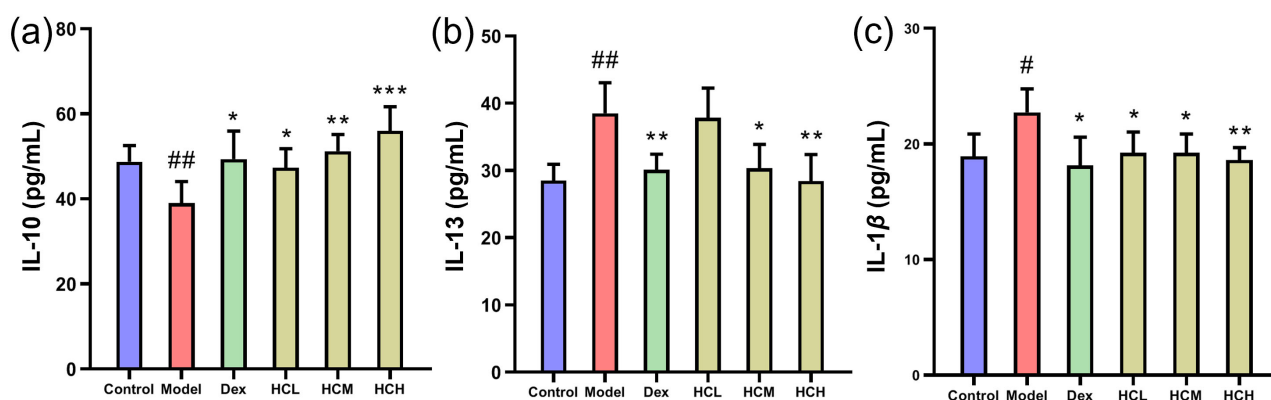


Fig. 3. Serum levels of inflammatory markers. (a) IL-10, (b) IL-13 and (c) IL-1 β in asthmatic rats treated with HC. Data are represented as Mean \pm SEM ($n = 8$), $^{\#}p < 0.05$, $^{##}p < 0.01$ vs Control group and $^*p < 0.05$, $^{**}p < 0.01$, $^{***}p < 0.001$ vs Model group.

nonpolar tissue samples underwent analysis using negative and positive ion modes, respectively (**Supplementary Fig. 2A–F**). Following data calibration and normalization, PCA analysis was performed using datasets from all samples.

The PCA score plots (**Supplementary Fig. 2G,H**) demonstrate tight clustering of QC samples in the center for both ion modes, suggesting good reproducibility and stability of the developed method.

The PCA score plots (Fig. 4a) revealed a basic separation between Control and Model groups. Furthermore, HCH group clustered closer to Control group compared to Model group. This suggested distinct metabolite profiles between Control and Model groups, with HCH group exhibiting more similarity to Control group. OPLS-DA yielded R2Y and Q2 values of 0.990 and 0.902 for Control-vs-Model (Fig. 4b), as well as 0.962 and 0.859 for HCH-vs-Model (Fig. 4d), consistently showed clear discrimination. Permutation tests confirmed the reliability of models, with R2 and Q2 values well below the original values (Fig. 4c,e). Based on the multivariate analysis of OPLS-DA (FC >1, VIP >1 and $p < 0.05$), 46 candidate serum metabolites were detected as potential biomarkers. These metabolites were primarily associated with lipid, organic acid, fatty acid and amino acid. Compared to Control group, 15 metabolites were up-regulated, while 31 were down-regulated in Model group. The HCH group exhibited 16 down-regulated and 19 up-regulated metabolites compared to the model group (Supplementary Table 3). The metabolite heatmap was shown in Fig. 4f.

Metabolic pathway analysis of the identified metabolites revealed distinct alterations across experimental groups. The Model group, compared to Control, exhibited remarkable enrichment in twelve key metabolic pathways, primarily related to lipid metabolism (glycerophospholipid, arachidonic acid, linoleic acid and sphingolipid), amino acid metabolism (arginine, proline, tyrosine, phenylalanine, tryptophan and beta-alanine) and energy metabolism (citrate cycle, pyruvate metabolism and purine metabolism) (Fig. 4g). Treatment with HCH partially reversed these, with 11 major pathways showing significant modulation, notably those associated with amino acid and energy metabolism (Fig. 4h).

To sum up, asthma induction disturbed these metabolic biomarkers as well as associated metabolic pathways. The alteration was mainly associated with lipid, amino acid and fatty acids metabolic disorders. After HCH intervention, the disorder reversed to some extent.

3.6 Transcriptomic Profile of HCH Treatment in OVA-Induced Asthma Model

The RNA-seq was performed on lung tissues from Control, Model and HCH groups to identify major DEGs and functional pathways involved in HCH action against OVA-induced allergic asthma. In Model-vs-Control group comparison, 754 DEGs were detected, with 454 up-regulated and 300 down-regulated. The HCH group exhibited 273 DEGs compared to Model group, of which 167 up-regulated and 106 down-regulated (Fig. 5a). The 20 most significantly enriched pathways of KEGG enrichment analysis are presented in Fig. 5b,c. In Model-vs-Control group, the most enriched pathways were primarily related to inflammation pathways (cytokine-cytokine receptor interaction, chemokine signaling pathway, TNF signaling

pathway and IL-17 signaling pathway), immune pathways (hematopoietic cell lineage, antigen processing and presentation, intestinal immune network for IgA production) and asthma. In Model-vs-Control and HCH-vs-Model groups, the enrichment pathways were mostly associated with airway mucus secretion (Hedgehog pathway), inflammation pathways (PI3K-Akt signaling pathway, MAPK signaling pathway, chemokine pathway, TNF signaling pathway and IL-17 signaling pathway) and airway remodeling (ECM-receptor interaction).

3.7 PPI Network Construction and Validation of Hub Genes Using RT-qPCR

According to the degree centrality, the PPI network analysis identified 6 genes with the highest degree values, including *Il6* (degree = 82), *Il10* (degree = 62), *Ccl2* (degree = 52), *Cxcl2* (degree = 34), *Ptgs2* (degree = 26) and *Cxcl6* (degree = 26), in the Model-vs-Control and HCH-vs-Model groups (Fig. 5d).

To validate the functions of HC in asthma by those potential hub genes, RT-qPCR was performed to assess *Il6*, *Il10*, *Ccl2*, *Cxcl2*, *Ptgs2* and *Cxcl6* mRNA expression (Fig. 6). The OVA-induced asthma resulted in a significant up-regulation of *Il6*, *Ccl2*, *Cxcl2*, *Ptgs2* and *Cxcl6* relative to Control group. Administration with HCH significantly down-regulated *Il6*, *Ccl2*, *Cxcl2* and *Cxcl6* expressions ($p < 0.05$). However, the *Ptgs2* expression did not change obviously and *Il10* was not detected.

3.8 Correlation Analysis of Metabolomics and Transcriptomics

To elucidate potential connections between DEGs and metabolic biomarkers, a gene-metabolite network was constructed using Metscape software (Supplementary Fig. 3). This analysis revealed seven key targets (*P4ha1*, *Pde3a*, *Pde5a*, *Adcy9*, *Pck2*, *Pla2g16* and *Entpd8*), corresponding to eleven differential metabolites (L-proline, L-arginine, L-malic acid, inosine, xanthosine, hypoxanthine, LysoPC(20:0), LysoPC(20:1(11Z)), arachidonic acid, PGE2 and PGF2a), involved in six important metabolic pathways (purine metabolism; arachidonic acid metabolism; urea cycle and metabolism of arginine, proline, glutamate, aspartate and asparagine; glycerophospholipid metabolism; glycolysis and gluconeogenesis; TCA cycle) in Model-vs-Control and HCH-vs-Model groups.

Spearman rank correlation was performed to assess the potential co-relationship between DEGs and differential metabolites. The analysis revealed potential correlations between DEGs and metabolites. Further analysis identified statistically significant correlations between some metabolites and DEGs (Fig. 7a). *P4ha1* was positively interrelated with L-proline and L-arginine ($p < 0.05$). *Pck2* showed a positive correlation with L-malic acid ($p < 0.01$). *Pde7b* was negatively interrelated with ADP ($p < 0.05$). *Adcy9* exhibited negative correlations with inosine, xanthosine and

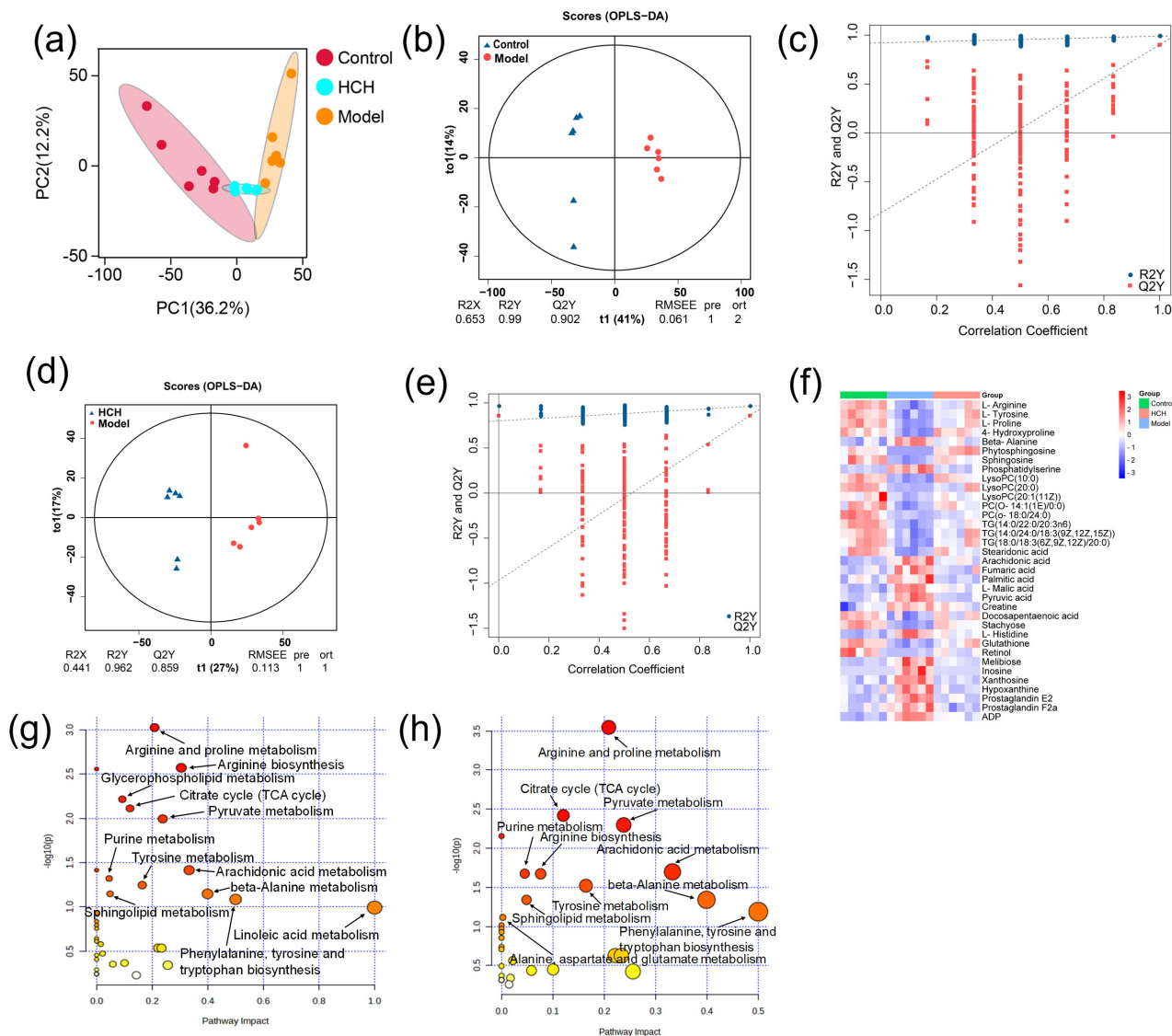


Fig. 4. Metabolomic profiling among the Control, Model and HCH groups. (a) Principal component analysis (PCA) score plot showcasing the overall separation of metabolic profiles. (b–e) Orthogonal projections to latent structures discriminant analysis (OPLS-DA) score plots depicting model validation and group separation. (f) Heatmap visualization of metabolic biomarkers among groups ($n = 6$) and (g,h) Metabolic pathway analysis of Model-vs-Control group, Model-vs-Control and HCH-vs-Model groups. (g,h) Size of the bubble corresponds to the pathway impact score and the color intensity represents the $-\log(p\text{-value})$.

hypoxanthine ($p < 0.05$). *Entpd8* showed positive correlations with inosine and xanthosine ($p < 0.01$ and $p < 0.05$). *Pde3a* was negatively interrelated with inosine and xanthosine ($p < 0.05$ and $p < 0.01$). *Pla2g16* exhibited negative correlations with LysoPC(20:0) and LysoPC(20:1(11Z)) ($p < 0.05$), while showing positive correlations with arachidonic acid, PGE2 and PGF2a ($p < 0.05$). *Ptgs2* displayed a positive correlation with arachidonic acid ($p < 0.05$). The *Pde3a* was negatively interrelated with inosine and xanthosine ($p < 0.05$ and $p < 0.01$). The *Pde5a* was negatively interrelated with hypoxanthine and xanthosine ($p < 0.05$). The *Rrm2b* displayed negative correlations with inosine and xanthosine ($p < 0.01$ and $p < 0.05$).

Furthermore, to evaluate the results of the network analysis, RT-qPCR was performed to verify the mRNA expression levels of those 10 genes in lung tissues (Fig. 7b). Compared with Control group, the expression of *P4hal*, *Pde3a*, *Pde5a*, *Pde7b* and *Adcy9* were notably reduced ($p < 0.05$). Conversely, the expression levels of *Ptgs2*, *Pck2*, *Pla2g16* and *Entpd8* were markedly elevated in Model group. The HCH group notably promoted the expression of *P4hal*, *Pde3a*, *Pde5a* and *Adcy9* and obviously inhibited the expression levels of *Pck2*, *Pla2g16* and *Entpd8* compared to the Model group. However, the mRNA levels of *Ptgs2* and *Pde7b* did not significantly improve. The changes of key metabolites and DEGs within five metabolic pathways identified in the analysis are shown in Fig. 8. It

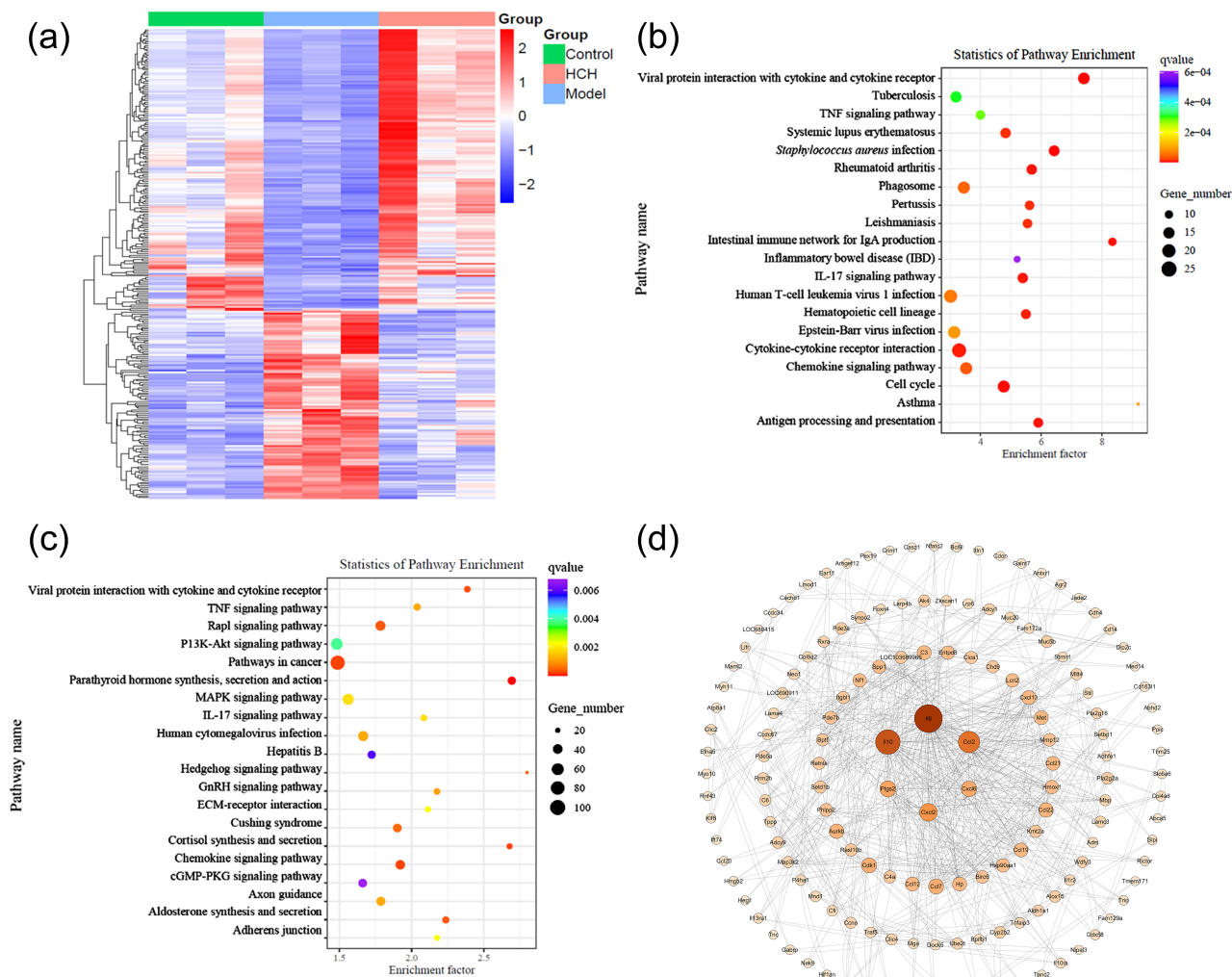


Fig. 5. Transcriptomic analysis revealing differentially expressed genes (DEGs), key pathways and hub genes modulated by HCH in the OVA-induced asthma model. (a) Heatmap showing DEGs in Control, Model and HCH groups. (b,c) Bubble chart showing Kyoto Encyclopedia of Genes and Genomes (KEGG) pathway enrichment analysis of DEGs in Model-vs-Control, HCH-vs-Model groups and (d) Protein-protein interaction (PPI) networks for DEGs in Model-vs-Control and HCH-vs-Model comparisons.

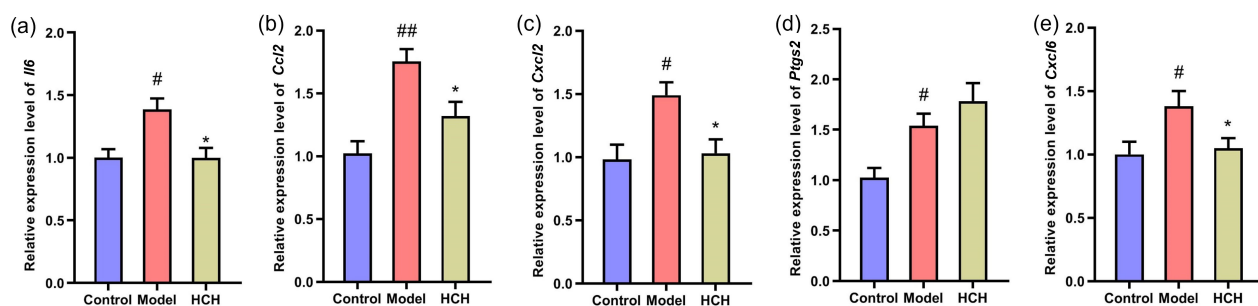


Fig. 6. Validation of hub gene expression by RT-qPCR. Relative mRNA expression levels of (a) *Il6*, (b) *Ccl2*, (c) *Cxcl2*, (d) *Ptgs2*, and (e) *Cxcl6* in the lung tissues of Control, Model, and HCH-treated rats. Results are represented by Mean \pm SEM (n = 3), # p < 0.05, ## p < 0.01 vs Control group and * p < 0.05 vs Model group.

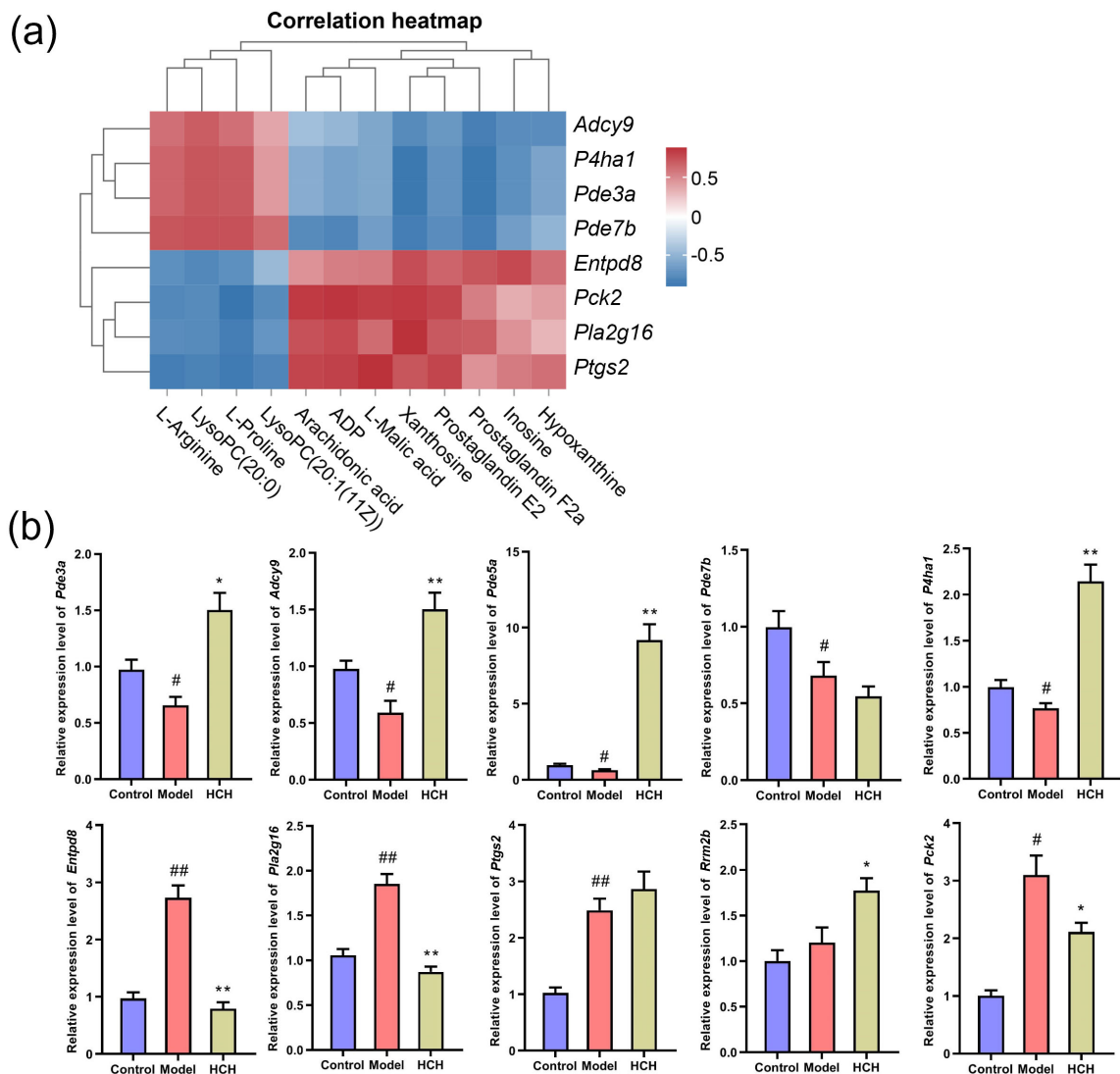


Fig. 7. Correlation analysis of metabolites, differentially expressed genes (DEGs) and validation of hub gene expression. (a) Significantly correlated metabolic biomarkers and DEGs and (b) RT-qPCR validation of 10 genes. Data are expressed as Mean \pm SEM ($n = 3$), # $p < 0.05$, ## $p < 0.01$ vs Control group and * $p < 0.05$, ** $p < 0.01$ vs Model group.

emphasizes the interconnectedness of metabolic and transcriptional responses and underscores HC's modulatory effects on these pathways.

4. Discussion

Analysis using the TCMSP database revealed that a majority of the 28 identified compounds were related to inflammatory diseases, indicating that HC may alleviate asthma by exerting anti-inflammatory effects. The H&E staining revealed HC effectively attenuated pulmonary inflammation. The ELISA assay showed that a high dose of HC down-regulated the expression of pro-inflammatory cytokines IL-13 and IL-1 β and up-regulated IL-10 expression and goblet cell proliferation was attenuated according to the PAS results, indicating that HC may exert anti-inflammatory properties by regulating IL-13, IL-1 β and IL-

10 expression and inhibit goblet cell proliferation to over-produce mucus by regulating IL-1 β and IL-13 expression.

Cytokines are well-established key players in asthma, contributing to AHR and airway blockage, mucus hyper-production and airway remodeling [45]. The PPI network analysis of DEGs identified several hub genes that are classified as cytokines (*Il6*, *Il10*, *Cxcl2*, *Cxcl6* and *Ccl2*) and *Ptgs2* plays a typical part in regulating inflammatory responses by producing prostaglandins [46], which indicates HC's therapeutic effects in allergic asthma may be closely associated with its anti-inflammatory effects.

The findings of this study reveal a remarkable metabolic and transcriptional feature in the lungs of asthmatic rats, with increased energy metabolism, reflected in both metabolite levels and gene expression (Fig. 8). Neutrophils have limited mitochondrial function and rely primarily on glycolysis and gluconeogenesis for ATP produc-

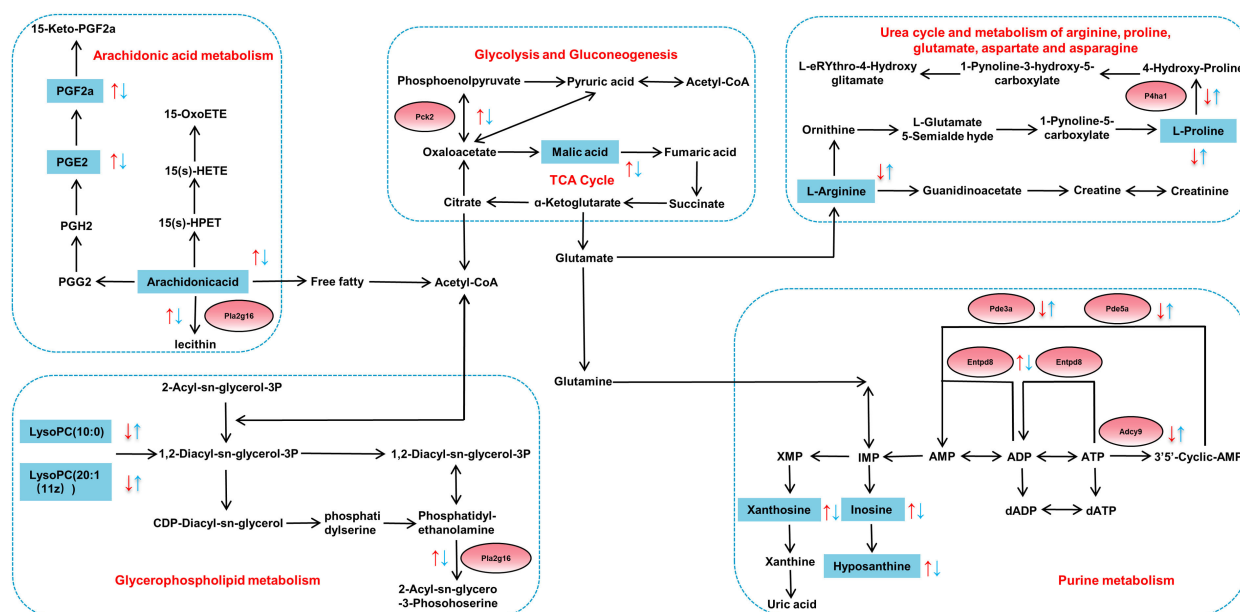


Fig. 8. Changes of metabolites (blue squares) and DEGs (red circles) within five metabolic pathways based on correlation analysis. Red arrows indicate increased/decreased levels in Model-vs-Control group and blue arrows represent increased/decreased levels in HCH-vs-Model group.

tion [52]. Previous research found that the intermediate products of aerobic oxidation in asthma patients who were in a state of hypoxia increased significantly, such as malic acid [53]. The up-regulated expression of *Pck2* and L-malic acid was restored after administration with a high dose of HC, which signified HC altered the state of hypoxia in asthmatic rats. Purine metabolism is essential for cellular energy homeostasis. Purine metabolites, including hypoxanthine, xanthine and inosine, were positively related to neutrophil inflammation in chronic obstructive pulmonary disease [49,54]. In current study, the elevated expression of inosine in asthmatic rats indicated a potential state of relative hypoxia and potential association with inflammatory processes. The up-regulated expression of *Entpd8*, xanthosine, hypoxanthine and inosine and the down-regulated expression of *Adcy9*, *Pde3a* and *Pde5a* were all restored after administration of HCH, which signified HC altered the abnormal energy metabolism of asthmatic rats.

The arachidonic acid metabolism pathway is a critical player in immune responses and inflammatory diseases (such as asthma). Arachidonic acid metabolites have been proposed as potential biomarkers for both diagnosis and treatment monitoring in allergic asthma and a new biological target for monitoring subcutaneous immunotherapy's therapeutic effect [55]. The PGE2 has been implicated in the exacerbation of several inflammatory responses and immune disorders [56]. The PGF2a has been linked to both acute and chronic inflammation [57]. Arachidonic acid represents the precursor to various strong pro-inflammatory [58]. In present study, HCH treatment also caused obvious decreased expression of arachidonic acid, PGE2, PGF2a

and *Pla2g16*, indicating that the inflammatory response in asthmatic rats was alleviated.

Glycerophospholipid metabolism has been implicated in the pathogenesis of OVA-induced allergic asthma [59, 60]. Lysophosphatidylcholines (LysoPCs) are reportedly decreased in asthmatic rats and may possess immunosuppressive properties [61]. Asthma is also associated with reduced systemic levels of L-arginine [62]. Administration of HCH reversed the up-regulated expression of *Pla2g16* and down-regulated the expression of *P4ha1*, L-proline, L-arginine, LysoPC(20:0) and LysoPC(20:1(11Z)), which revealed HC altered the abnormal of glycerophospholipid metabolism, glycolysis and gluconeogenesis.

5. Conclusion

Our findings demonstrated that HC treatment effectively inhibited airway inflammation and mucus hypersecretion in OVA-induced asthma. Integrative analysis of transcriptomic and metabolomic data suggested that HC may alleviate asthma by modulating energy metabolism and the inflammatory response. These results provide novel insights into the therapeutic mechanism of HC in asthma, potentially contributing to future pharmacological research and clinical applications on more effective herbal-based therapies for asthma.

Availability of Data and Materials

The datasets used and analyzed during the current study are available from the corresponding author on reasonable request.

Author Contributions

RW and SW conceived and designed the research study and methodology. RW, XS, XD, LH, and ZL performed the research and investigation. GJ provided validation, provided help and advice on the experiments. RW, XS, and ZL performed the formal analysis, software analysis, and data curation. XD and LH drafted the original manuscript. RW, XS and SW reviewed and edited the manuscript. SW provided supervision, project administration, and funding acquisition. All authors contributed to editorial changes in the manuscript. All authors read and approved the final manuscript. All authors have participated sufficiently in the work and agreed to be accountable for all aspects of the work.

Ethics Approval and Consent to Participate

All animal experimentation procedures adhered to the guidelines and were approved by the Animal Ethics Committee of Changchun University of Chinese Medicine (protocol no.: 2020345; approval date: October 11, 2020).

Acknowledgment

Not applicable.

Funding

This research was supported by the Jilin Province Science and Technology Development Plan Project (192485YY010358427).

Conflict of Interest

The authors declare no conflict of interest.

Supplementary Material

Supplementary material associated with this article can be found, in the online version, at <https://doi.org/10.31083/IJP44196>.

References

- [1] Krusche J, Twardziok M, Rehbach K, Böck A, Tsang MS, Schröder PC, *et al.* TNF- α -induced protein 3 is a key player in childhood asthma development and environment-mediated protection. *The Journal of Allergy and Clinical Immunology*. 2019; 144: 1684–1696.e12. <https://doi.org/10.1016/j.jaci.2019.07.029>.
- [2] Bradding P, Porsbjerg C, Côté A, Dahlén SE, Hallstrand TS, Brightling CE. Airway hyperresponsiveness in asthma: The role of the epithelium. *Journal of Allergy and Clinical Immunology*. 2024; 153: 1181–1193. <https://doi.org/10.1016/j.jaci.2024.02.011>.
- [3] Gillissen A, Paparoupa M. Inflammation and infections in asthma. *The Clinical Respiratory Journal*. 2015; 9: 257–269. <https://doi.org/10.1111/crj.12135>.
- [4] Corren J. Role of interleukin-13 in asthma. *Current Allergy and Asthma Reports*. 2013; 13: 415–420. <https://doi.org/10.1007/s11882-013-0373-9>.
- [5] Erle DJ, Sheppard D. The cell biology of asthma. *The Journal of Cell Biology*. 2014; 205: 621–631. <https://doi.org/10.1083/jcb.201401050>.
- [6] Fahy JV. Type 2 inflammation in asthma—present in most, absent in many. *Nature Reviews. Immunology*. 2015; 15: 57–65. <https://doi.org/10.1038/nri3786>.
- [7] Lim JCW, Goh FY, Sagineedu SR, Yong ACH, Sidik SM, Lajis NH, *et al.* A semisynthetic diterpenoid lactone inhibits NF- κ B signalling to ameliorate inflammation and airway hyperresponsiveness in a mouse asthma model. *Toxicology and Applied Pharmacology*. 2016; 302: 10–22. <https://doi.org/10.1016/j.taap.2016.04.004>.
- [8] Wills-Karp M. Interleukin-13 in asthma pathogenesis. *Current Allergy and Asthma Reports*. 2004; 4: 123–131. <https://doi.org/10.1007/s11882-004-0057-6>.
- [9] Simpson JL, Phipps S, Baines KJ, Oreo KM, Gunawardhana L, Gibson PG. Elevated expression of the NLRP3 inflammasome in neutrophilic asthma. *The European Respiratory Journal*. 2014; 43: 1067–1076. <https://doi.org/10.1183/09031936.00105013>.
- [10] Besnard AG, Togbe D, Couillin I, Tan Z, Zheng SG, Erard F, *et al.* Inflammasome-IL-1-Th17 response in allergic lung inflammation. *Journal of Molecular Cell Biology*. 2012; 4: 3–10. <https://doi.org/10.1093/jmcb/mjr042>.
- [11] Zhang Y, Xu CB, Cardell LO. Long-term exposure to IL-1 β enhances Toll-IL-1 receptor-mediated inflammatory signaling in murine airway hyperresponsiveness. *European Cytokine Network*. 2009; 20: 148–156. <https://doi.org/10.1684/ecn.2009.0156>.
- [12] Urry Z, Xystrakis E, Hawrylowicz CM. Interleukin-10-secreting regulatory T cells in allergy and asthma. *Current Allergy and Asthma Reports*. 2006; 6: 363–371. <https://doi.org/10.1007/s11882-996-0005-8>.
- [13] Rose MC, Voynow JA. Respiratory tract mucin genes and mucin glycoproteins in health and disease. *Physiological Reviews*. 2006; 86: 245–278. <https://doi.org/10.1152/physrev.00010.2005>.
- [14] Mukherjee AA, Kandhare AD, Rojatkhar SR, Bodhankar SL. Ameliorative effects of *Artemisia pallens* in a murine model of ovalbumin-induced allergic asthma via modulation of biochemical perturbations. *Biomedicine & Pharmacotherapy*. 2017; 94: 880–889. <https://doi.org/10.1016/j.biopha.2017.08.017>.
- [15] Bateman ED, Hurd SS, Barnes PJ, Bousquet J, Drazen JM, FitzGerald JM, *et al.* Global strategy for asthma management and prevention: GINA executive summary. *The European Respiratory Journal*. 2008; 31: 143–178. <https://doi.org/10.1183/09031936.00138707>.
- [16] Ji W, Zhang Q, Shi H, Dong R, Ge D, Du X, *et al.* The mediatory role of Majie cataplasm on inflammation of allergic asthma through transcription factors related to Th1 and Th2. *Chinese Medicine*. 2020; 15: 53. <https://doi.org/10.1186/s13020-020-00334-w>.
- [17] Dong Y, Yan H, Zhao X, Lin R, Lin L, Ding Y, *et al.* Gu-Ben-Fang-Xiao Decoction Ameliorated Murine Asthma in Remission Stage by Modulating Microbiota-Acetate-Tregs Axis. *Frontiers in Pharmacology*. 2020; 11: 549. <https://doi.org/10.3389/fphar.2020.00549>.
- [18] Lo PC, Lin SK, Lai JN. Long-term use of Chinese herbal medicine therapy reduced the risk of asthma hospitalization in school-age children: A nationwide population-based cohort study in Taiwan. *Journal of Traditional and Complementary Medicine*. 2019; 10: 141–149. <https://doi.org/10.1016/j.jtcme.2019.04.005>.
- [19] Arora D, Sharma A. A review on phytochemical and pharmacological potential of genus *Chelidonium*. *Pharmacognosy Journal*. 2013; 5: 184–190. <https://doi.org/10.1016/j.phcgg.2013.07.006>.
- [20] Colombo ML, Bosisio E. Pharmacological activities of *Chelidonium majus* L. (Papaveraceae). *Pharmacological Research*. 1996; 33: 127–134. <https://doi.org/10.1006/phrs.1996.0019>.

- [21] Mikołajczak PŁ, Kędzia B, Ożarowski M, Kujawski R, Bogacz A, Bartkowiak-Wieczorek J, *et al.* Evaluation of anti-inflammatory and analgesic activities of extracts from herb of *Chelidonium majus* L. Central-European Journal of Immunology. 2015; 40: 400–410. <https://doi.org/10.5114/ceji.2015.54607>.
- [22] Stancic-Rotaru M, Mititelu M, Crasmaru M, Balaban D. Spectroanalytical profile of flavonoids from *Chelidonium majus* L. Romanian Biotechnological Letters. 2002; 8: 1093–1100.
- [23] Park JE, Cuong TD, Hung TM, Lee I, Na M, Kim JC, *et al.* Alkaloids from *Chelidonium majus* and their inhibitory effects on LPS-induced NO production in RAW264.7 cells. Bioorganic & Medicinal Chemistry Letters. 2011; 21: 6960–6963. <https://doi.org/10.1016/j.bmcl.2011.09.128>.
- [24] Kuenzel J, Geisler K, Strahl O, Grundtner P, Beckmann MW, Dittrich R. *Chelidonium majus* and its effects on uterine contractility in a perfusion model. European Journal of Obstetrics, Gynecology, and Reproductive Biology. 2013; 169: 213–217. <https://doi.org/10.1016/j.ejogrb.2013.03.014>.
- [25] Monavari SH, Shahrabadi MS, Keyvani H, Bokharaei-Salim F. Evaluation of in vitro antiviral activity of *Chelidonium majus* L. against herpes simplex virus type-1. African Journal of Microbiology Research. 2012; 6: 4360–4364. <https://doi.org/10.5897/AJMR11.1350>.
- [26] Pan J, Yang Y, Zhang R, Yao H, Ge K, Zhang M, *et al.* Enrichment of chelidonine from *Chelidonium majus* L. using macroporous resin and its antifungal activity. Journal of Chromatography. B, Analytical Technologies in the Biomedical and Life Sciences. 2017; 1070: 7–14. <https://doi.org/10.1016/j.jchromb.2017.10.029>.
- [27] Khodabande Z, Jafarian V, Sariri R. Antioxidant activity of *Chelidonium majus* extract at phenological stages. Applied Biological Chemistry. 2017; 60: 497–503. <https://doi.org/10.1007/s13765-017-0304-x>.
- [28] Hiller KO, Ghorbani M, Schilcher H. Antispasmodic and relaxant activity of chelidonine, protopine, coptisine, and *Chelidonium majus* extracts on isolated guinea-pig ileum. Planta Medica. 1998; 64: 758–760. <https://doi.org/10.1055/s-2006-957576>.
- [29] Song JY, Yang HO, Pyo SN, Jung IS, Yi SY, Yun YS. Immunomodulatory activity of protein-bound polysaccharide extracted from *Chelidonium majus*. Archives of Pharmacological Research. 2002; 25: 158–164. <https://doi.org/10.1007/BF02976557>.
- [30] Capistrano I R, Wouters A, Lardon F, Gravekamp C, Apers S, Pieters L. In vitro and in vivo investigations on the antitumour activity of *Chelidonium majus*. Phytomedicine: International Journal of Phytotherapy and Phytopharmacology. 2015; 22: 1279–1287. <https://doi.org/10.1016/j.phymed.2015.10.013>.
- [31] Liao W, He X, Yi Z, Xiang W, Ding Y. Chelidonine suppresses LPS-Induced production of inflammatory mediators through the inhibitory of the TLR4/NF- κ B signaling pathway in RAW264.7 macrophages. Biomedicine & Pharmacotherapy. 2018; 107: 1151–1159. <https://doi.org/10.1016/j.biopha.2018.08.094>.
- [32] Kim SH, Hong JH, Lee YC. Chelidonine, a principal isoquinoline alkaloid of *Chelidonium majus*, attenuates eosinophilic airway inflammation by suppressing IL-4 and eotaxin-2 expression in asthmatic mice. Pharmacological Reports: PR. 2015; 67: 1168–1177. <https://doi.org/10.1016/j.pharep.2015.04.013>.
- [33] Wang R, Sui X, Dong X, Hu L, Li Z, Yu H, *et al.* Integration of metabolomics and transcriptomics reveals the therapeutic mechanism underlying *Chelidonium majus* L. in the treatment of allergic asthma. Chinese Medicine. 2024; 19: 65. <https://doi.org/10.1186/s13020-024-00932-y>.
- [34] Wu X, Wang S, Lu J, Jing Y, Li M, Cao J, *et al.* Seeing the unseen of Chinese herbal medicine processing (*Paozhi*): advances in new perspectives. Chinese Medicine. 2018; 13: 4. <https://doi.org/10.1186/s13020-018-0163-3>.
- [35] Li RL, Zhang Q, Liu J, He LY, Huang QW, Peng W, *et al.* Processing methods and mechanisms for alkaloid-rich Chinese herbal medicines: A review. Journal of Integrative Medicine. 2021; 19: 89–103. <https://doi.org/10.1016/j.joim.2020.12.003>.
- [36] Chen LL, Verpoorte R, Yen HR, Peng WH, Cheng YC, Chao J, *et al.* Effects of processing adjuvants on traditional Chinese herbs. Journal of Food and Drug Analysis. 2018; 26: S96–S114. <https://doi.org/10.1016/j.jfda.2018.02.004>.
- [37] Pan L, Wang Y, Yue L, Wang N, Xu W, Liao X, *et al.* Review on Processing Methods of Toxic Chinese Materia Medica and the Related Mechanisms of Action. The American Journal of Chinese Medicine. 2023; 51: 1385–1412. <https://doi.org/10.1142/S0192415X23500635>.
- [38] Chen Z, Ye SY, Zhu RG. The extraordinary transformation of traditional Chinese medicine: processing with liquid excipients. Pharmaceutical Biology. 2020; 58: 561–573. <https://doi.org/10.1080/13880209.2020.1778740>.
- [39] Hussein SZ, Mohd Yusoff K, Makpol S, Mohd Yusof YA. Gelam Honey Inhibits the Production of Proinflammatory Mediators NO, PGE(2), TNF- α , and IL-6 in Carrageenan-Induced Acute Paw Edema in Rats. Evidence-based Complementary and Alternative Medicine: ECAM. 2012; 2012: 109636. <https://doi.org/10.1155/2012/109636>.
- [40] Mohd Zohdi R, Abu Bakar Zakaria Z, Yusof N, Mohamed Mustapha N, Abdullah MNH. Gelam (*Melaleuca* spp.) Honey-Based Hydrogel as Burn Wound Dressing. Evidence-based Complementary and Alternative Medicine: ECAM. 2012; 2012: 843025. <https://doi.org/10.1155/2012/843025>.
- [41] Yao LK, Razak SLA, Ismail N, Fai NC, Asgar MHAM, Sharif NM, *et al.* Malaysian gelam honey reduces oxidative damage and modulates antioxidant enzyme activities in young and middle aged rats. Journal of Medicinal Plant Research. 2011; 5: 5618–5625.
- [42] Mokhtar N, Chan SC. Use of complementary medicine amongst asthmatic patients in primary care. The Medical Journal of Malaysia. 2006; 61: 125–127.
- [43] Liu M, Yang Z, Wen J, Ma Z, Sun L, Wang M, *et al.* The effect of honey as an excipient in the processing of traditional Chinese medicine based on chemical profiling, artificial neural network, and virtual screening: Cortex Mori as an example. Arabian Journal of Chemistry. 2024; 17: 105519. <https://doi.org/10.1016/j.arabjc.2023.105519>.
- [44] Li T, Li H, Zhong L, Qin Y, Guo G, Liu Z, *et al.* Analysis of heterologous expression of phaCBA promotes the acetoin stress response mechanism in *Bacillus subtilis* using transcriptomics and metabolomics approaches. Microbial Cell Factories. 2024; 23: 58. <https://doi.org/10.1186/s12934-024-02334-z>.
- [45] Wishart DS, Feunang YD, Marcu A, Guo AC, Liang K, Vázquez-Fresno R, *et al.* HMDB 4.0: the human metabolome database for 2018. Nucleic Acids Research. 2018; 46: D608–D617. <https://doi.org/10.1093/nar/gkx1089>.
- [46] Sumner LW, Amberg A, Barrett D, Beale MH, Beger R, Daykin CA, *et al.* Proposed minimum reporting standards for chemical analysis Chemical Analysis Working Group (CAWG) Metabolomics Standards Initiative (MSI). Metabolomics: Official Journal of the Metabolomic Society. 2007; 3: 211–221. <https://doi.org/10.1007/s11306-007-0082-2>.
- [47] Suzuki ÉY, Simon A, da Silva AL, Amaro MI, de Almeida GS, Agra LC, *et al.* Effects of a novel roflumilast and formoterol fumarate dry powder inhaler formulation in experimental allergic asthma. International Journal of Pharmaceutics. 2020; 588: 119771. <https://doi.org/10.1016/j.ijpharm.2020.119771>.
- [48] Hellmann J, Tang Y, Zhang MJ, Hai T, Bhatnagar A, Srivastava S, *et al.* Atf3 negatively regulates Ptg2/Cox2 expression during

- acute inflammation. Prostaglandins & Other Lipid Mediators. 2015; 116–117: 49–56. <https://doi.org/10.1016/j.prostaglandins.2015.01.001>.
- [49] Hatse S, De Clercq E, Balzarini J. Role of antimetabolites of purine and pyrimidine nucleotide metabolism in tumor cell differentiation. Biochemical Pharmacology. 1999; 58: 539–555. [https://doi.org/10.1016/s0006-2952\(99\)00035-0](https://doi.org/10.1016/s0006-2952(99)00035-0).
- [50] Wang M, Ren C, Wang P, Cheng X, Chen Y, Huang Y, *et al.* Microbiome-Metabolome Reveals the Contribution of the Gut-Testis Axis to Sperm Motility in Sheep (*Ovis aries*). Animals. 2023; 13: 996. <https://doi.org/10.3390/ani13060996>.
- [51] Yang C, Wu P, Yao X, Sheng Y, Zhang C, Lin P, *et al.* Integrated Transcriptome and Metabolome Analysis Reveals Key Metabolites Involved in *Camellia oleifera* Defense against Anthracnose. International Journal of Molecular Sciences. 2022; 23: 536. <https://doi.org/10.3390/ijms23010536>.
- [52] Liu TT, Wang YL, Zhang Z, Jia LX, Zhang J, Zheng S, *et al.* Abnormal adenosine metabolism of neutrophils inhibits airway inflammation and remodeling in asthma model induced by *Aspergillus fumigatus*. BMC Pulmonary Medicine. 2023; 23: 258. <https://doi.org/10.1186/s12890-023-02553-x>.
- [53] Wolak JE, Esther CR, Jr, O'Connell TM. Metabolomic analysis of bronchoalveolar lavage fluid from cystic fibrosis patients. Biomarkers: Biochemical Indicators of Exposure, Response, and Susceptibility to Chemicals. 2009; 14: 55–60. <https://doi.org/10.1080/13547500802688194>.
- [54] Esther CR, Jr, Coakley RD, Henderson AG, Zhou YH, Wright FA, Boucher RC. Metabolomic Evaluation of Neutrophilic Airway Inflammation in Cystic Fibrosis. Chest. 2015; 148: 507–515. <https://doi.org/10.1378/chest.14-1800>.
- [55] Zheng P, Bian X, Zhai Y, Li C, Li N, Hao C, *et al.* Metabolomics reveals a correlation between hydroxyeicosatetraenoic acids and allergic asthma: Evidence from three years' immunotherapy. Pediatric Allergy and Immunology. 2021; 32: 1654–1662. <https://doi.org/10.1111/pai.13569>.
- [56] Tsuge K, Inazumi T, Shimamoto A, Sugimoto Y. Molecular mechanisms underlying prostaglandin E2-exacerbated inflammation and immune diseases. International Immunology. 2019; 31: 597–606. <https://doi.org/10.1093/intimm/dxz021>.
- [57] Basu S. Bioactive eicosanoids: role of prostaglandin F(2 α) and F₂-isoprostanes in inflammation and oxidative stress related pathology. Molecules and Cells. 2010; 30: 383–391. <https://doi.org/10.1007/s10059-010-0157-1>.
- [58] Pedersen SF, Poulsen KA, Lambert IH. Roles of phospholipase A2 isoforms in swelling- and melittin-induced arachidonic acid release and taurine efflux in NIH3T3 fibroblasts. American Journal of Physiology. Cell Physiology. 2006; 291: C1286–C1296. <https://doi.org/10.1152/ajpcell.00325.2005>.
- [59] Wang S, Tang K, Lu Y, Tian Z, Huang Z, Wang M, *et al.* Revealing the role of glycerophospholipid metabolism in asthma through plasma lipidomics. Clinica Chimica Acta; International Journal of Clinical Chemistry. 2021; 513: 34–42. <https://doi.org/10.1016/j.cca.2020.11.026>.
- [60] Quinn KD, Schedel M, Nkrumah-Elie Y, Joetham A, Armstrong M, Cruickshank-Quinn C, *et al.* Dysregulation of metabolic pathways in a mouse model of allergic asthma. Allergy. 2017; 72: 1327–1337. <https://doi.org/10.1111/all.13144>.
- [61] Yu M, Cui FX, Jia HM, Zhou C, Yang Y, Zhang HW, *et al.* Aberrant purine metabolism in allergic asthma revealed by plasma metabolomics. Journal of Pharmaceutical and Biomedical Analysis. 2016; 120: 181–189. <https://doi.org/10.1016/j.jpba.2015.12.018>.
- [62] Winnica D, Que LG, Baffi C, Grasemann H, Fiedler K, Yang Z, *et al.* L-citrulline prevents asymmetric dimethylarginine-mediated reductions in nitric oxide and nitrosative stress in primary human airway epithelial cells. Clinical and Experimental Allergy. 2017; 47: 190–199. <https://doi.org/10.1111/cea.12802>.